RETRIEVED ICE MICROPHYSICS FROM CALIPSO AND CLOUDSAT AND HORIZONTALLY ORIENTED ICE PLATES

Hajime Okamoto[1], Kaori Sato[1], Yuichiro Hagihara[1] , Takuya Matsumoto[1] and Anatoli Borovoi[2]

[1]*Research Institute for Applied Mechanics, Kyushu University, Kasuga park 6-1, Kasuga, Fukuoka, Japan, okamoto@riam.kyushu-u.ac.jp*

[2]*V.E. Zuev Institute of Atmospheric Optics, Rus. Acad. Sci., I., Academician Zuev Sq., Tomsk 634021, Russia, borovoi@iao.ru*

ABSTRACT

We improved the radar and lidar algorithm that can be applied to CloudSat and Cloud-Aerosol Lidar and Infrared Pathfinder Satellite Observations (CALIPSO) data to retrieve ice microphysics. The essential modification is the implementation of distribution of tilt angles of ice plates respect to the horizontal plane. We introduced the Gauss-type and Klett-type distribution functions in the improved version of the algorithm. The backscattering signatures in radar and lidar wavelengths were calculated for the same particle type and orientation by using the discrete dipole approximation and physical optics, respectively.

Introducing the distribution of orientations lead to the large reduction of lidar backscattering coefficient compared with that for perfectly oriented ice plates with same effective radius and mass but larger than that for spheres for the CALIPSO tilt angle of 0.3°.

The effective radius and ice water content were similar between the improved and old algorithms. Mass fraction of oriented crystals to the total IWC became much larger in the improved algorithms when the specular reflection was observed.

1. INTRODUCTION

The CloudSat and CALIPSO satellites were launched in April 2006 and have been operational since June 2006. CloudSat carries a cloud profiling radar that measures the radar reflectivity factor at 95GHz. The CALIPSO carries a lidar that can measure the attenuated backscattering coefficient at 532nm and 1064nm and the depolarization ratio at 532nm. Scattering properties of particles vary with wavelength. Radar signals are larger for larger size with the same ice water content (IWC) and lidar signals are smaller for spherical particles with the same IWC. Lidar signals for non-spherical particles show the strong dependence on particle shape. Due to the differences for the size dependences between the radar and lidar wavelengths, it became possible to retrieve ice effective radius and IWC by the combined use of the measurements of CloudSat and CALIPSO. However, there are several important issues in the analysis of cloud microphysics. One of the issues is related to the analysis of specular reflections in the lidar signals. When the particles tend to be oriented in horizontal plane, the lidar backscattering can become much stronger than that for the randomly oriented crystals. Without the explicit treatment of such phenomena, the retrieved ice microphysics may contain significant errors. CALIPSO has a capability to measure the depolarization ratios (δ) and this parameter has been known to be an indicator of non-spherical particles. In the space borne lidar measurements, the spherical water particles can produce large depolarization ratios due to the multiple scattering effects when optical thickness is sufficiently large. Consequently, the low δ with low attenuation corresponds to the existence of oriented ice plate-type [1]. The combination of δ and attenuation can be used to infer the vertically resolved cloud particle types [2]. The frequent occurrence of oriented ice plates was found between -10°C to -20°C. And larger occurrence of plates was found at higher latitudes. There are several radar-lidar algorithms [3-6] and only two of the algorithms can treat the clouds that show specular reflection in the lidar signals [5,6]. In the algorithm, we used Ze at 95GHz from CloudSat and β and δ at 532nm from CALIPSO to study cloud microphysics. The mixture of randomly oriented ice and horizontally oriented ice were considered. For the plate-type, the perfect orientation in the horizontal plane was assumed in the original version of the algorithm. Global analyses of ice cloud microphysics have been provided. Here, we introduced the distribution of tilt angle for oriented plates in the improved algorithm and the impact of the modification in the retrieved ice microphysics was examined.

2. THEORETICAL PROCEDURE

Before applying the radar-lidar algorithm to ice cloud microphysics retrievals, the determination of grid boxes that contain cloud particles in ice phase was needed. We used the cloud mask scheme developed in [7] for the CloudSat and CALIPSO data. The method used the threshold to discriminate cloud from aerosols developed in ship-based measurements [8] and also a spatial continuity test.

Then the cloud particle types were determined as follows. The polarization capability of lidar provides δ, defined as a ratio of backscatters in the planes of polarization perpendicular and parallel to the linearly polarized incident beam. The δ has been used to infer ice particles habits. In case of space borne lidar such as CALIPSO, the water clouds tend to exhibit significant δ owning to the multiple scattering [1] when the optical thickness is large. In addition to δ, we introduced a new parameter estimated from two attenuated backscattering coefficients in neighboring layers. The combination of these parameters enables discrimination between water and ice particles. Ice is further categorized into randomly oriented ice crystals (3-D ice) and 2-D plate [2].

For the ice microphysics retrievals, we considered the coexistence of 3D-ice and plate categories in the same cloud layers. The mixture of 50% of horizontally oriented column and 50% of bullet-rosette (CB50) were considered as 3D-ice [9]. For the plate category, we consider the distribution of tilt angles relative to the horizontal plane (hereafter quasi-2D-plate). The distribution was described by Gauss or Klett type functions [10]. The standard deviation of the tilt angle was prescribed in the Gauss type distribution. In the Klett type distribution function, the temperature, pressure, energy dissipation rate, particle terminal velocity are needed. Thus the orientation depended on the particle size in Klett model. The lidar backscattering due to the oriented plates has been studied [11-13]. To estimate the lidar backscattering signals, we must use the physical optics rather than the simple application of ray tracing approach. For the 95GHz cloud radar signals, we applied the discrete dipole approximation to take into account the particle shape and orientations.

The size distribution was assumed to be a modified Gamma distribution [14]. Then we prepared the look up tables (LUTs) where β and extinction coefficient at 532nm and Ze for constant IWC were tabulated for various effective radii. CALIPSO pointed in near nadir direction before 28 November 2007. Since then, to avoid the specular reflection often observed, the instrument has been pointed 3^{o} off nadir. We prepared LUTs for each case.

From the observed β and δ at 532nm and Ze at 95GHz, effective radius, IWC and fraction of IWC for quasi-2D-plate type to the total IWC were retrieved by the algorithm.

3. THEORETICAL RESULTS OF β

We showed β at 532nm for IWC=1[g/m^3] for various effective radius for the lidar tilt angle of 0.3^{o}. The 2D-plate(specular) denotes the plates with perfect horizontal orientation and internal and corner reflection were neglected. The 2D-plate (all) corresponded to the same particle geometry as the 2D-plate(specular) but the internal reflection between the top and bottom surfaces were considered and corner reflection from sides was not included. The plates with Gauss distribution with the standard deviation of 1^{o} was denoted as plate-Gauss,all model. The internal reflection was taken into account. The plates with the Klett distribution with the energy dissipation rate of 100 was denoted as plate-Klett,all where internal reflection was included. For the comparisons, CB50 model and the sphere model were also shown (Figure 1).

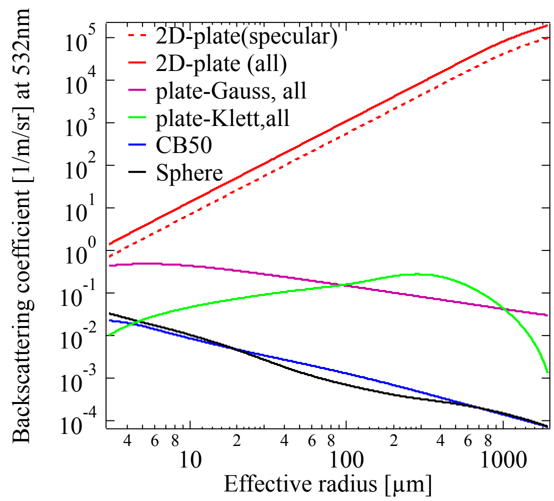

Figure 1. The lidar backscattering coefficient β [1/m/sr] for ice plates with perfect orientation and two distribution models of tilt angle for IWC=1g/m^{3} as function of effective radius [μm]. Lidar tilt angle was set to be 0.3^{o} off nadir.

The 2D-plate (all) model showed the largest β among the models. The inclusion of the distribution of tilt angles of plates lead to reduce β compared with the perfectly oriented plates. The differences between the Gauss and Klett-distribution were also large, especially for small particles. The plate-Klett model showed smaller β for small particles because the fraction of large tilt angle respect to the horizontal plane was larger in Klett model than that for Gauss model and the resultant β became smaller for Klett distribution for effective radius<100μm. For larger effective radius, the fraction of large tilt angle in Klett distribution was smaller and β became larger compared with the Gauss distribution. The β also showed dependences on the parameters used to describe Gauss and Klett model. Since these parameters have to be prescribed in the LUTs in the retrieval algorithms, this could be the source of uncertainties in the retrieved cloud microphysics. The β for plates with several distribution functions of the tile angle showed larger than those for CB50 and spheres for effective radius >10μm. Thus, it was shown that specular reflection occurred for the existence of plates in the clouds layers for lidar tilt angle of 0.3 ^{o}.

4. RETRIEVAL RESULTS OF CLOUD MICROPHYSICS AND DISCUSSIONS

The improved algorithm was applied to the CloudSat and CALIPSO data. The retrieval results of effective radius, IWC and the fraction of quasi-2D-plate are shown in Figure 2. The data were taken on 8 October 2006 in the area 30^{o}S-60^{o}S, 114^{o}W-123^{o}W. The lower layers showed large β corresponding to specular reflection and small δ at around 4-5km. And the cloud particle type algorithm classified the layer to be oriented plates. The effect radius was lager than 150μm and often exceeded 200μm in the layers, while effective radius in upper layers showed smaller values of around 30μm (Figure 2a). IWC showed slightly larger values in the region of specular reflections than in the upper layers (Figure 2b). The results from the improved algorithm showed large fraction of quasi-2D-plates, e.g., exceed 50% in some specular reflection regions (white color) and small values in upper regions where no specular reflection occurred (Figure 2c). In contrast, the old algorithm with perfect oriented plate model showed less than 0.1% of the fraction of plates (not shown). The Klett model was also used to retrieve cloud microphysics. The differences between the Gauss and Klett-models were very small for effective radius and IWC and were also small for the fraction of plates.

The one to one comparisons between the improved and old algorithms were carried out. The effective radius and IWC were similar between the improved and old algorithms. The retrieved fraction of quasi-2D plates by the improved algorithm was almost three orders larger than that by the old algorithm (Figure 3). These similarities and differences between the improved and old algorithms could be understood as follows; the old algorithm only retrieved the fraction of perfectly oriented plates and the fraction was small compared with the total fraction of plates, i.e., most of the plates were not perfectly oriented in horizontal plane. On the other hand, the β for perfectly oriented plates were much larger than that of non-perfectly oriented plates. Thus the old algorithm failed to account the actual fraction of oriented plates but could adequately take into account the total enhancement of backscattering due to the plates. Consequently, the retrieved effective radius and IWC were estimated correctly by the old algorithm.

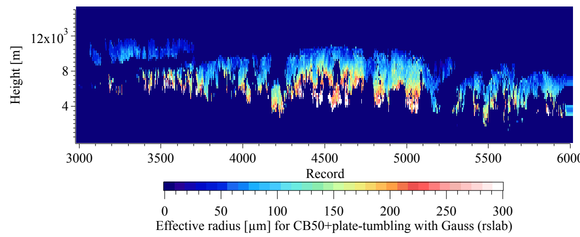

(a)

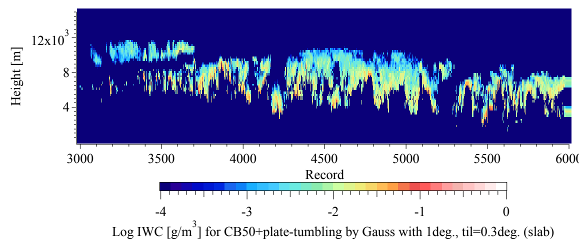

(b)

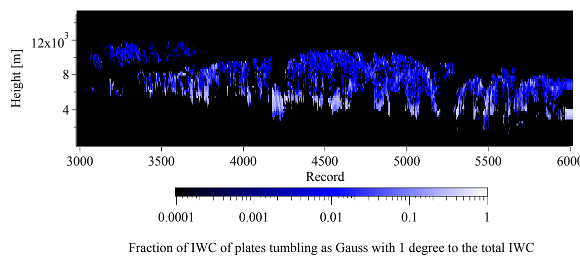

(c)

Figure 2 (a) Retrieved effective radius of ice clouds containing specular reflection by the improved algorithm. (b) retrieved IWC, (c) retrieved fraction of IWC of quasi-2D plates to the total IWC. The vertical and horizontal axes denote height and record. The observed data corresponded to the area 30oS-60S, 114oW-123W on 8 October 2006.

The value of the fraction of quasi-2D plates seemed to be larger than the previously reported values in the literature where the area-weighted fraction retrieved by the POLDER lies between 0.1 to 1% [15]. The reason for the discrepancies might be explained as follows; the analyses of the POLDER were limited to the cloud top portions. Contrary, in our lidar analyses, high fraction of quasi-oriented plates were found in the lower portion of cloud layers and top portions contained small fraction of plates where the cold temperatures <-20 ^{o}C and there was not many occurrence of plates in the temperature range.

The EarthCARE is ESA-JAXA mission and will carry Doppler cloud radar and high spectral resolution lidar. It is noted that extension of the algorithm for the EarthCARE is straightforward.

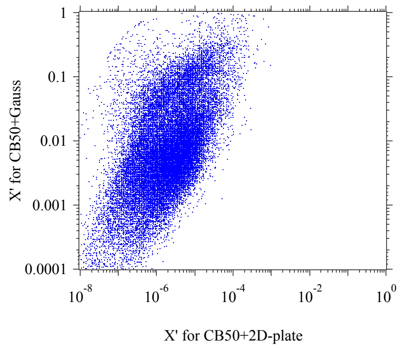

Figure 3 Comparison of fraction of plates for the improved (vertical) and old algorithms (horizontal).

ACKNOWLEDGMENTS

We thank CloudSat and CALIPSO science teams for providing the data used here. This work was supported by the Ministry of Education, Culture, Sports, Science and Technology of Japan through Grants-in-Aid for Scientific Research B (22340133) and by GRENE Arctic Climate Change Research Project.. K. Sato was supported by the Grant in Aid for Young Scientists (B) (23740358) and Supporting positive activities for female researchers, Special Coordination Funds for Promoting Science and Technology, Ministry of Education, Culture, Sports, Science and Technology and Kyushu University Interdisciplinary Programs in Education and Projects in Research Development (P&P). A. Borovoi is acknowledged to Kyushu University where he was affiliated as a visiting researcher.

REFERENCES

1. Hu, Y. 2007: Depolarization ratio-effective lidar ratio relation: Theoretical basis for space lidar cloud phase discrimination, *Geophys. Res. Lett.,* **34**, L11812, doi:10.1029/2007GL029584.

2. Yoshida, R., H. Okamoto, Y. Hagihara, and H. Ishimoto, 2010: Global analysis of cloud phase and ice crystal orientation from Cloud-Aerosol Lidar and Infrared Pathfinder Satellite Observation (CALIPSO) data using attenuated backscattering and depolarization ratio, *J. Geophys. Res.,* **115**, D00H32, doi:10.1029/2009JD012334.

3. Delanoë, J., and R. J. Hogan, 2010: Combined CloudSat-CALIPSO-MODIS retrievals of the properties of ice clouds, *J. Geophys. Res.*, **115**, D00H29, doi:10.1029/2009JD012346.

4. Deng, M., G. G. Mace, Z. Wang, and H. Okamoto, 2010: TC4 validation for ice cloud profiling retrieval using CloudSat radar and CALIPSO lidar, *J. Geophys. Res.* **115**, D00J15, doi:10.1029/2009JD013104.

5. Okamoto, H., K. Sato, and Y. Hagihara, 2010: Global analysis of ice microphysics from CloudSat and CALIPSO: Incorporation of specular reflection in lidar signals, *J. Geophys. Res.*, **115**, D22209, doi:10.1029/2009JD013383.

6. Sato, K. and H. Okamoto, 2011: Refinement of global ice microphysics using spaceborne active sensors, *J. Geophys. Res.*, **116**, doi:10.1029/2011JD015885.

7. Hagihara, Y., H. Okamoto, and R. Yoshida, 2010: Development of a combined CloudSat/CALIPSO cloud mask to show global cloud distribution, *J. Geophys. Res*., **115**, doi:10.1029/2009JD012344.

8. Okamoto, H., et al. 2007: Vertical cloud structure observed from ship- borne radar and lidar: Midlatitude case study during the MR01/K02 cruise of the research vessel Mirai, *J. Geophys. Res.*, **112**, D08216, doi:10.1029/2006JD007628.

9. Sato, K., and H. Okamoto, 2006: Characterization of Ze and LDR of non-spherical and inhomogeneous ice particles for 95-GHz cloud radar: Its implication to microphysical retrievals, *J. Geophys. Res.*, **111**, D22213-doi:10.1029/2005JD006959.

10. Klett, J. D. 1995: Orientation model for particles in turbulence, *J. Atmos. Sci.*, **52**, pp. 2276–2285

11. Borovoi A., G., I. A. Grishin, 2003: Scattering matrices for large ice crystal particles, *J. Opt. Soc. Am.,* **20A**, pp. 2071-2080.

12. Iwasaki, S., and H. Okamoto, 2001: Analysis of the enhancement of the backscattering by non-spherical particles with flat surfaces, *Appl. Opt.*, **40**, 6121–6129.

13. Mishchenko, M. I., D. J. J. Wielaard, and B. E. Carlson, 1997: T-matrix computations of zenith-enhanced lidar backscatter from horizontally ori- ented ice plates, *Geophys. Res. Lett.*, **24**, 771–774, doi:10.1029/ 97GL00545.

14. Okamoto, H., S. Iwasaki, M. Yasui, H. Horie, H. Kuroiwa, and H. Kumagai, 2003: An algorithm for retrieval of cloud microphysics using 95-GHz cloud radar and lidar, *J. Geophys. Res.*, **108(D7)**, 4226, doi:10.1029/ 2001JD001225.

15. Breon, F.-M, B. Dubrulle, 2004: Horizontally oriented plates in clouds, *J. Atmos. Sci.*, **61**, pp. 2888-2898.